



Broadband mid-infrared pulse via intra-pulse difference frequency generation based on supercontinuum from multiple thin plates

Hang-Dong Huang(黄杭东), Chen-Yang Hu(胡晨阳), Hui-Jun He(何会军), Hao Teng(滕浩), Zhi-Yuan Li(李志远), Kun Zhao(赵昆), Zhi-Yi Wei(魏志义)

Citation: Chin. Phys. B . 2019, 28(11): 114203 . **doi:** 10.1088/1674-1056/ab4579

Journal homepage: <http://cpb.iphy.ac.cn>; <http://iopscience.iop.org/cpb>

What follows is a list of articles you may be interested in

Atomic even-harmonic generation due to symmetry-breaking effects induced by spatially inhomogeneous field

Yue Guo(郭月), Aihua Liu(刘爱华), Jun Wang(王俊), Xueshen Liu(刘学深)

Chin. Phys. B . 2019, 28(9): 094212 . **doi:** 10.1088/1674-1056/ab37fa

Generation of few-cycle radially-polarized infrared pulses in a gas-filled hollow-core fiber

Rui-Rui Zhao(赵睿睿), Zhi-Yuan Huang(黄志远), Ding Wang(王丁), Yu Zhao(赵钰), Yu-Xin Leng(冷雨欣), Ru-Xin Li(李儒新)

Chin. Phys. B . 2018, 27(10): 104204 . **doi:** 10.1088/1674-1056/27/10/104204

Self-compression of 1.8- μ m pulses in gas-filled hollow-core fibers

Rui-Rui Zhao(赵睿睿), Ding Wang(王丁), Yu Zhao(赵钰), Yu-Xin Leng(冷雨欣), Ru-Xin Li(李儒新)

Chin. Phys. B . 2017, 26(10): 104206 . **doi:** 10.1088/1674-1056/26/10/104206

Two-dimensional materials for ultrafast lasers

Fengqiu Wang(王枫秋)

Chin. Phys. B . 2017, 26(3): 034202 . **doi:** 10.1088/1674-1056/26/3/034202

Mid-IR dual-wavelength difference frequency generation in uniform grating PPLN using index dispersion control

Chang Jian-Hua, Sun Qing, Ge Yi-Xian, Wang Ting-Ting, Tao Zai-Hong, Zhang Chuang

Chin. Phys. B . 2013, 22(12): 124204 . **doi:** 10.1088/1674-1056/22/12/124204

Broadband mid-infrared pulse via intra-pulse difference frequency generation based on supercontinuum from multiple thin plates*

Hang-Dong Huang(黄杭东)^{1,2}, Chen-Yang Hu(胡晨阳)^{2,3}, Hui-Jun He(何会军)^{2,3}, Hao Teng(滕浩)², Zhi-Yuan Li(李志远)⁴, Kun Zhao(赵昆)^{2,†}, and Zhi-Yi Wei(魏志义)^{2,3,‡}

¹School of Physics and Optoelectronic Engineering, Xidian University, Xi'an 710071, China

²Beijing National Laboratory for Condensed Matter Physics, Institute of Physics, Chinese Academy of Sciences, Beijing 100190, China

³University of Chinese Academy of Sciences, Beijing 100049, China

⁴College of Physics and Optoelectronics, South China University of Technology, Guangzhou 510640, China

(Received 4 August 2019; revised manuscript received 8 September 2019; published online 18 October 2019)

We report on the generation of optical pulses with a nearly one octave-spanning spectrum ranging from 1300 nm to 2500 nm at 1 kHz repetition rate, which are based on intra-pulse difference frequency generation (DFG) in β -barium borate crystal (β -BBO) and passively carrier-envelope-phase (CEP) stabilized. The DFG is induced by few-cycle pulses initiated from spectral broadening in multiple thin plates driven by a Ti: sapphire chirped-pulse amplifier. Furthermore, a numerical simulation is developed to estimate the conversion efficiency and output spectrum of the DFG. Our results show that the pulses from the DFG have the potential for seeding intense mid-infrared (MIR) laser generation and amplification to study strong-field physics and attosecond science.

Keywords: infrared pulses, difference frequency generation, ultrafast laser

PACS: 42.65.Re, 95.85.Jq, 52.35.Mw

DOI: 10.1088/1674-1056/ab4579

1. Introduction

In recent years, remarkable progress in the generation of intense laser pulses has opened new fields in attosecond science, strong field physics, time-resolved spectroscopy, and nonlinear optics.^[1–4] Among these important applications, high energy few-cycle laser pulses in the mid-infrared (MIR) region with stabilized carrier-envelope phase (CEP) are considered as the optimal drivers for high photon energy isolated attosecond pulse generation.^[5,6] Currently, such pulses with center wavelength near 1.8 μm have already enabled the generation of attosecond pulses in the soft x-ray water window.^[7–9] The generation of pulse with 53-as duration was reported in 2017.^[10] Up to now, isolated attosecond pulses as short as 43-as experimentally generated by utilizing intense two cycle driving pulses around the central wavelength of 1.8 μm have been demonstrated.^[11]

Compared with pulses from mode-locked lasers directly, three-wave mixing method such as optical parametric amplification (OPA) or optical parametric chirped pulse amplification (OPCPA) is an alternative and more effective way of generating high energy ultrafast MIR pulses near 2 μm .^[12,13] A sufficient seed bandwidth is a critical prerequisite to achieve an ultra-broadband output spectrum in OPA or OPCPA. Consequently, intra-pulse difference frequency generation (DFG) is proposed and employed as the MIR seeding source for several

features, including more than one octave broad phase matching bandwidth, no jitter between the pump and the signal, and passively stabilized CEP for the idler since the pump and the signal are within the same pulse.^[14–16]

Achieving such tunable MIR lasers via intra-pulse DFG typically requires an ultra-broadband spectrum from the supercontinuum generation (SCG) process. The mainstream technique to generate few-cycle pulses is to broaden the spectrum of multi-cycle pulses from laser amplifiers through inert-gas-filled hollow-core fibers (HCFs) and compress the pulse width with chirped mirrors.^[17,18] Nevertheless, such process requires pulses with energy on the order of mJ, and the transmission is usually only $\sim 50\%$ primarily caused by multiphoton processes and waveguide mode selection.^[19] In addition, SCG based on HCFs requires a strict beam stability for injecting the laser pulse into the several-hundred-micron core of the fiber.

Recently, a novel technique containing multiple thin plates has been developed to efficiently increase the bandwidth of high energy multi-cycle laser pulses as an alternative to generating filamentation in an HCF.^[20,21] It has been reported in a variety of spectral range covering 400 nm to 3500 nm and pulse energy from the level of hundreds of μJ to a few of mJ.^[22–26] The spectrum of the driving laser is broadened by self-phase modulation (SPM), self-steepening, and self-focusing in an ar-

*Project supported by the National Key R&D Program of China (Grant No. 2017YFB0405202), the Major Program of the National Natural Science Foundation of China (Grant No. 61690221), the Key Program of the National Natural Science Foundation of China (Grant No. 11434016), and the National Natural Science Foundation of China (Grant Nos. 11574384 and 11674386).

†Corresponding author. E-mail: zhaokun@iphy.ac.cn

‡Corresponding author. E-mail: zywei@iphy.ac.cn

ray of strategically positioned thin plates. This multi-plate scheme is applicable with a broad range of input energy in various materials, simultaneously offering transmittance higher than 85%.^[27] Furthermore, such a multi-plate system offers high stability and good mode quality, while the advantages of compactness and operational simplicity are preserved.

In this paper, a broadband MIR pulse generated via intra-pulse DFG in β -barium borate crystal (β -BBO) is put forward, which is driven by few-cycle pulses obtained through spectral broadening in multiple thin plates. The DFG pulse has a broad spectrum covering from 1300 nm to 2500 nm with passively stabilized CEP. This system can endure variable input energy and produce broadband MIR pulses. In addition to the experimental results, a numerical simulation is developed to estimate the conversion efficiency and output spectrum of the DFG.

2. Experimental setup and results

Figure 1 shows the experimental setup. The optical setup mainly consists of two parts: (A) SCG source and pulse compression, (B) intra-pulse DFG in a nonlinear crystal. In the SCG part, the driving source is a mode-locked Ti: sapphire laser with chirped pulse amplification (CPA) by a multi-pass amplifier, whose spectrum is presented with a dashed line in Fig. 2(a). The pulse energy is about 800 μ J at a repetition rate of 1 kHz with a pulse width of 30 fs (full width at half maximum, FWHM). To obtain an SCG, the seed femtosecond laser pulse at 500 μ J is focused into seven pieces of thin fused silica with thickness of 100 μ m by an $f = 2000$ mm lens, and the output beam is collimated by a concave mirror with a focal length of 1000 mm. In this configuration, the pulse spectrum broadens sequentially in each plate and acquires a nonlinear phase sufficient for self-focusing. Several materials have been utilized in our experiment, such as fused silica, sapphire, and YAG, and fused silica shows the best performance among them. The beam size within the Rayleigh length and the position of the silica are the two keys during the SCG. By adjusting the parameter of the focusing lens, the focal beam diameter is around 600 μ m, corresponding to a peak laser power density of 1×10^{13} W/cm². To avoid damage and ionization, the silica is kept away from the focal point and the positions of the plates are subtly chosen by compromising between the maximum spectral widths and transmission efficiency. Compared with traditional HCFs, SCG by multiple thin plates is more compact and can support mJ injected pulse energy with high beam quality, which is a considerable advantage in our experiment for further OPCPA or OPA development.

The spectrum of SCG is shown with a solid line in Fig. 2(a), covering from 500 nm to 900 nm, which is equivalent to that of a Fourier-transform-limited (FTL) pulse with a 7.1 fs pulse width, as shown in Fig. 2(b). The SCG is compressed to sub-10 fs pulses with 350 μ J by a set of chirped

mirrors. A concave silver mirror with radius of curvature of 1000 mm is used to focus the incident beam to 200 μ m in diameter at the focal point. A BBO crystal is chosen as the DFG medium for its high transparency in the visible and IR spectral ranges with high nonlinearity and high damage threshold. The DFG takes place in the 0.5 mm thick β -BBO crystal for type II phase-matching, e.g., 600 nm (e) \rightarrow 900 nm (e) + 1800 nm (o). To obtain the DFG spectrum, a piece of Si as a band pass filter (BPF) is used to remove the residual driving pulse.

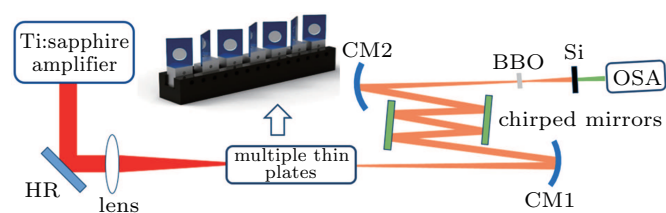


Fig. 1. Schematic diagram of the experimental setup. HR: high reflection-coated mirror; CM1 and CM2: concave mirrors with silver coating; OSA: optical spectral analyzer.

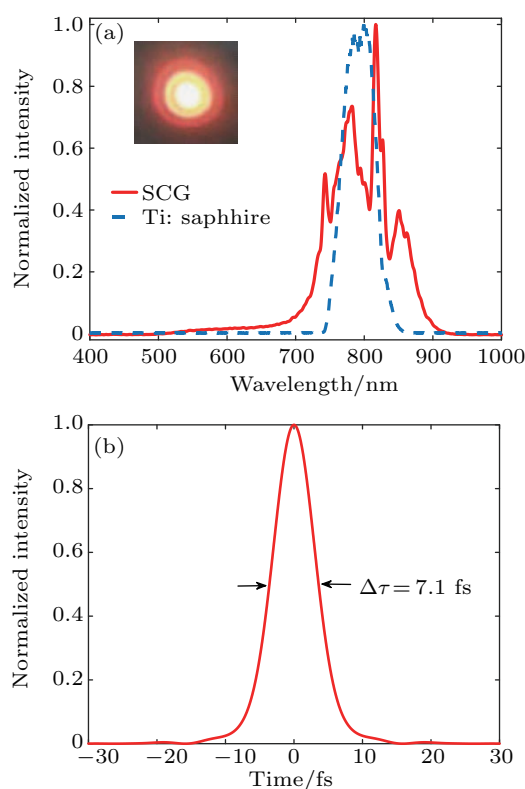


Fig. 2. (a) Solid line: SCG after seven fused silica plates; dashed line: spectrum of Ti: sapphire CPA. Inset: the output beam profile taken before the collimating mirror. (b) Transform-limited pulse duration of 7.1 fs from the SCG.

To determine the crystal cutting angle, phase-matching conditions with different angles of 32°, 34°, 36°, and 38° are shown in Fig. 3. The horizontal and vertical axes are the components of the driving pulse. The color bar indicates the phase-matching efficiency determined by $\text{sinc}(\Delta kL/2)$, where Δk denotes the phase-mismatch per unit length and L is the length of the BBO crystal. The dark blue region denotes the

phase-matched area, corresponding to high phase-matching efficiency. The solid color lines indicate different idler wavelengths. If the lines pass through the phase-matched region, it indicates that this particular angle of the crystal supports effective production of the idle wavelength. More lines pass through the blue area, broader DFG spectrum the crystal angle supports. In our experiment, the spectrum of the driving pulses covers 500 nm to 950 nm. Considering the spectrum of the driving source, we add a dashed line to show the actually working region. The region above the dash line will take place in our situation while below will not. From Figs. 3(a)–3(d),

the blue area becomes narrower with the angle increasing from 32° to 38°, which means that the bandwidth of DFG decreases. For example, the DFG spectrum near 2400 nm will not be generated in the BBO crystal with a cutting angle of 32° based on our simulation. On the other hand, the blue area moves toward the short wavelength side along the vertical axis, showing that the overall efficiency rises since the blue area grows large. Considering the spectrum of the driving pulse, the blue area of 36° is larger than that of 38°, so we choose the cutting angle of the BBO crystal at 36°.

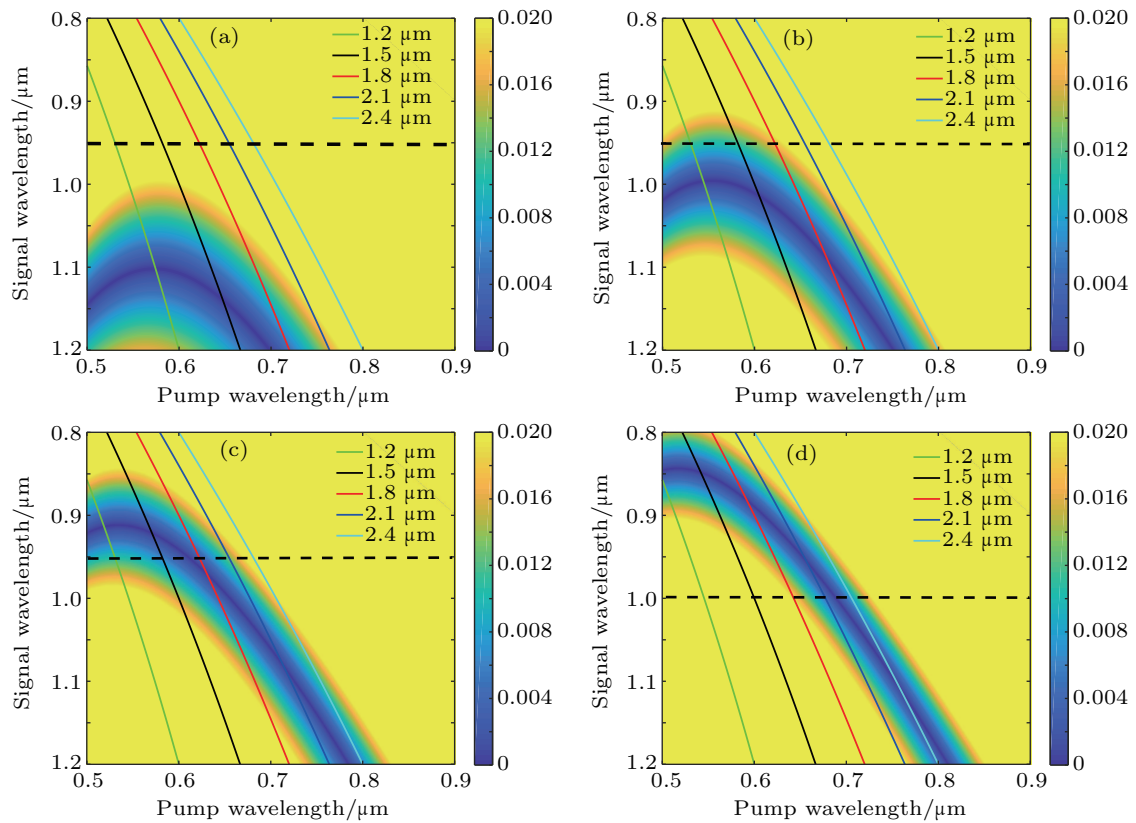


Fig. 3. Phase mismatch diagrams at different phase matching angles: (a) 32°, (b) 34°, (c) 36°, and (d) 38°.

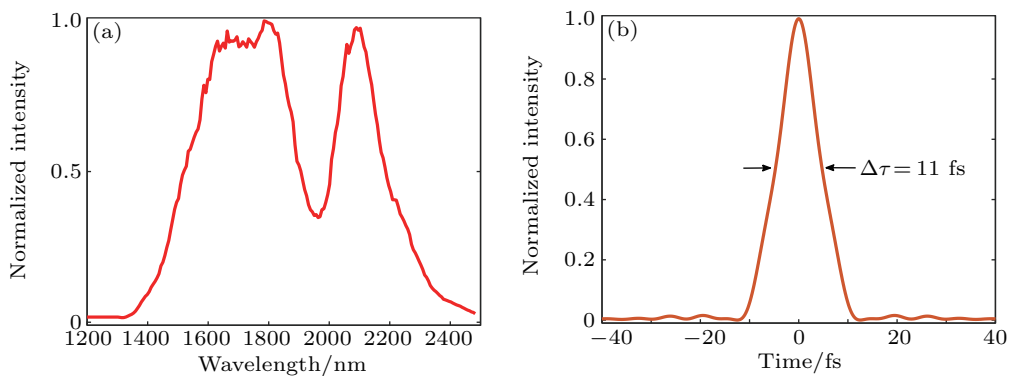


Fig. 4. (a) DFG spectrum. (b) Transform-limited pulse duration of 11 fs from the DFG spectrum.

By optimizing the angle and position of the BBO crystal, near octave-spanning MIR DFG pulses are generated and measured by an optical spectral analyzer (Ocean Optics, NIR-

Quest). Due to the measurement range of the spectral analyzer, the DFG spectrum is limited to 1300 nm to 2500 nm, as illustrated in Fig. 4(a). Figure 4(b) shows the calculated FTL pulse

with a duration of 11 fs that contains a 1.8 cycle carrier at the central wavelength of 1800 nm.

3. Numerical simulation and results

The energy of the DFG signal in our experiment is at nJ level. To investigate the impact of different phase-matching conditions, we develop a numerical simulation to illustrate the phase-matching process and evaluate the output bandwidth and conversion efficiency by solving a series of coupled wave equations in frequency domain. At first, we split the spectrum of the pump, signal, and idler waves into discrete parts by means of discrete Fourier transform. Then, we rewrite the second order nonlinear polarization. For each individual frequency component, the corresponding nonlinear polarization is involved in a series of terms under the law of energy conservation, which indicate the coupled nonlinear interactions. Assuming all series of mixing waves are plane waves, we derive the following equations from Maxwell equations:

$$\frac{dE_i^{\text{pump}}(\omega_i)}{dz} = \frac{i\omega_i}{2n(\omega_i)c} d_{\text{eff}} \sum_{\omega_j}^{N_2} \sum_{\omega_k}^{N_3} E_j^{\text{sig}}(\omega_j) E_k^{\text{idle}*}(\omega_k) \times e^{i(k_i - k_j - k_k)z} \delta_{\omega_k, \omega_i - \omega_j}, \quad (1)$$

$$\frac{dE_j^{\text{sig}}(\omega_j)}{dz} = \frac{i\omega_j}{2n(\omega_j)c} d_{\text{eff}} \sum_{\omega_i}^{N_1} \sum_{\omega_k}^{N_3} E_i^{\text{pump}}(\omega_i) E_k^{\text{idle}*}(\omega_k) \times e^{i(k_i - k_j - k_k)z} \delta_{\omega_k, \omega_i - \omega_j}, \quad (2)$$

$$\frac{dE_k^{\text{idle}}(\omega_k)}{dz} = \frac{i\omega_k}{2n(\omega_k)c} d_{\text{eff}} \sum_{\omega_i}^{N_1} \sum_{\omega_j}^{N_2} E_i^{\text{pump}}(\omega_i) E_j^{\text{sig}*}(\omega_j) \times e^{i(k_i - k_j - k_k)z} \delta_{\omega_k, \omega_i - \omega_j}, \quad (3)$$

where

$$\delta_{\omega_k, \omega_i + \omega_j} = \begin{cases} 1, & \omega_k = \omega_i - \omega_j, \\ 0, & \omega_k \neq \omega_i - \omega_j, \end{cases}$$

E is the electric-field amplitude, d_{eff} is the effective second-order nonlinearity, ω is the angular frequency, n is the refractive index, and c is the light speed in vacuum. The contribution of each nonlinear process is determined by the corresponding phase-matching condition and the amplitude of the corresponding electric field. By taking Sellmeier equation of the BBO into these equations, the method can be applied to evaluate the conversion efficiency and the output spectrum of DFG. Considering the transmission window of the BBO crystal, the spectra and efficiencies of DFG from numerical simulations are shown in Fig. 5(a) under different phase-matching conditions with cutting angles of 32° , 34° , 36° , and 38° . It should be pointed out that the vertical axis in Fig. 5 is normalized for different phase-matching conditions.

From Fig. 5(a), the width of the spectrum increases with the cutting angle. It is consistent with the variation of the blue area shown in Fig. 3. However, the FWHM of the spectrum increases from 32° to 36° , and decreases when the cutting angle

further increases to 38° . It is due to that the efficiency has a remarkable increase when the cutting angle is 38° as shown in Fig. 5. This increase of efficiency is mainly concentrated near the central wavelength. The progressive increase in efficiency with increasing cutting angle can be explained by that the blue area moves toward the short wavelength side along the vertical axis, approaching the 800 nm waveband as shown in Fig. 3. The main intensity of the driving source is around 800 nm. Therefore, the process of DFG can be enhanced. To produce higher energy DFG, one may increase the thickness and use a medium with higher nonlinearity, or increase the energy in the long and short wavelength sides in the driving pulse. Besides, increasing the peak power of the incident pulse may be useful as well.

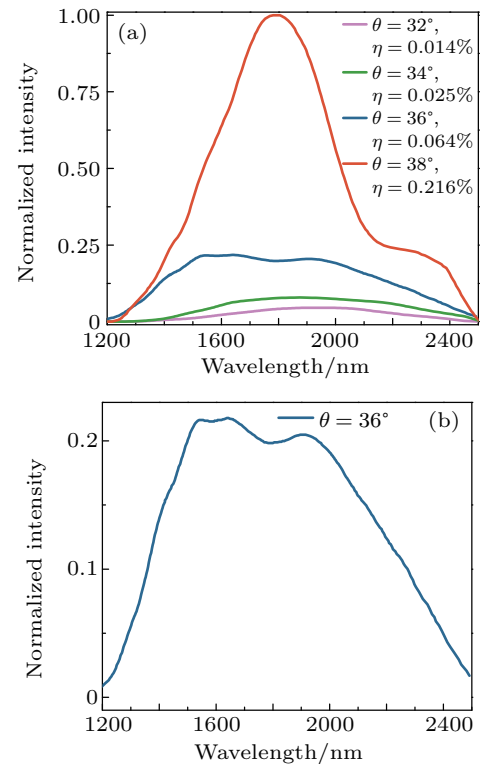


Fig. 5. (a) Spectra and efficiencies of DFG from numerical simulations at different phase matching angles. (b) The shape detail of the spectrum of 36° .

Though high efficiency can enhance the process of DFG, greater FWHM of the spectrum is a more critical parameter which is beneficial for further research. Overall considering, the spectrum and efficiency of DFG of 36° cutting angle are optimized. In Fig. 5(b), the shape of the spectrum of DFG of 36° is shown. It reveals that the numerical simulation at 36° has a good agreement with the shape of the spectrum in our experimental result as shown in Fig. 4(a).

4. Conclusion and perspectives

In summary, ultra-broadband MIR pulses initiated from intra-pulse DFG in BBO crystal are experimentally investigated. Instead of traditional HCFs, multiple thin plates are uti-

lized to generate SCG based on a Ti: sapphire CPA to support such tunable MIR pulses. This scheme is compact and adaptable with various energy and wavelength of the injected laser pulses, which are non-sensitive to the pointing stability of the driving laser. It is a useful tool to realize the wavelength conversion and pulse compression in ultrafast optics field. A BBO crystal at 36° cutting angle is chosen for the type II phase-matching interaction. The spectrum of DFG covers an octave from 1300 nm to 2500 nm, which supports an FTL pulse of 11 fs width. In addition, a numerical simulation is developed to estimate the conversion efficiency and output spectrum of the DFG, which matches our experimental result well and has significant impact on designing and improving experiments and optical components in nonlinear optics research. Due to the broad spectrum and passively stabilized CEP, the intrapulse DFG derived from the multiple-plate scheme is versatile as a promising candidate in seeding a high-energy OPCPA or OPA for further applications in studying strong field physics and attosecond science.

References

- [1] Brabec T and Krausz F 2000 *Rev. Mod. Phys.* **72** 545 1
- [2] Tittel F K, Richter D and Fried A 2003 *Solid-State Mid-Infrared Laser Sources* (Berlin, Heidelberg: Springer) p. 458
- [3] Goulielmakis E, Schultze M, Hofstetter M, Yakovlev V S, Gagnon J, Uiberacker M, Aquila A L, Gullikson E M, Attwood D T, Kienberger R, Krausz F and Kleineberg U 2008 *Science* **320** 1614
- [4] Chang Z H, Corkum P B and Leone S R 2016 *J. Opt. Soc. Am. B* **33** 1081
- [5] Zhao K, Zhang Q, Chini M, Wu Y, Wang X W and Cang Z H 2012 *Opt. Lett.* **37** 3891
- [6] Wu Y, Cunningham E, Zang H, Li J, Chini M, Wang X, Wang Y, Zhao K and Chang Z 2013 *Appl. Phys. Lett.* **102** 201104
- [7] Ishii N, Kaneshima K, Kitano K, Kanai T, Watanabe S and Itatani J 2014 *Nat. Commun.* **5** 3331
- [8] Silva F, Teichmann S M, Cousin S L, Hemmer M and Biegert J 2015 *Nat. Commun.* **6** 6611
- [9] Li J, Ren X M, Yin Y C, Cheng Y, Cunningham E, Wu Y and Cang Z H 2016 *Appl. Phys. Lett.* **108** 231102
- [10] Li J, Ren X M, Yin Y C, Zhao K, Chew A, Cheng Y, Cunningham E, Wang Y, Hu S Y, Wu Y, Chini M and Chang Z H 2017 *Nat. Commun.* **8** 186
- [11] Gaumnitz T, Jain A, Pertot Y, Huppert M, Jordan I, Ardana-Lamas F and Wörner H J 2017 *Opt. Express* **25** 27506
- [12] Ishii N, Kaneshima K, Kitano K, Kanai T, Watanabe S and Itatani J 2012 *Opt. Lett.* **37** 4182
- [13] Hong K H, Lai C J, Siqueira J P, Krogen P, Moses J, Chang C L, Stein G J, Zapata L E and Kärtner F X 2014 *Opt. Lett.* **39** 3145
- [14] Fuji T, Ishii N, Teisset C Y, Gu X, Metzger T and Baltuška A 2006 *Opt. Lett.* **31** 1103
- [15] Yin Y C, Ren X M, Chew A, Li J, Wang Y, Zhuang F J, Wu Y and Chang Z H 2017 *Sci. Rep.* **7** 11097
- [16] Ren X M, Mach L H, Yin Y C, Wang Y and Chang Z H 2018 *Opt. Lett.* **43** 3381
- [17] Hort O, Dubrouil A, Cabasse A, Petit P, Mével E, Descamps D and Constant E 2015 *J. Opt. Soc. Am. B* **32** 1055
- [18] Yin Y C, Li J, Ren X M, Wang Y, Chew A and Chang Z H 2016 *Opt. Lett.* **41** 1142
- [19] Cardin V, Thiré N, Beaulieu S, Wanie V, Légaré F and Schmidt B E 2015 *Appl. Phys. Lett.* **107** 181101
- [20] Lu C H, Tsou Y J, Chen H Y, Chen B H, Cheng Y C, Yang S D, Chen M C, Hsu C C and Kung A H 2014 *Optica* **1** 400
- [21] Lu C H, Witting T, Husakou A, Vrakking Marc J J, Kung A H and Furch F J 2018 *Opt. Express* **26** 8941
- [22] Hwang S I, Park S B, Mun J, Cho W, Nam C H and Kim K T 2019 *Sci. Rep.* **9** 1613
- [23] Lu F M, Xia P Y, Matsumoto Y, Kanai T, Ishii N and Itatani J 2018 *Opt. Lett.* **43** 2720
- [24] Canhota M, Weig R and Crespo H M 2019 *Opt. Lett.* **44** 1015
- [25] Lu C H, Wu W H, Kuo S H, Guo J Y, Chen M C, Yang S D and Kung A H 2019 *Opt. Express* **27** 15638
- [26] Liu Y Y, Zhao K, He P, Huang H D, Teng H and Wei Z Y 2017 *Chin. Phys. Lett.* **34** 074204
- [27] He P, Liu Y Y, Zhao K, Teng H, He X K, Huang P, Huang H D, Zhong S Y, Jiang Y J, Fang S B, Hou X and Wei Z Y 2017 *Opt. Lett.* **42** 474